Inorganic Chemistry

Article

pubs.acs.org/IC

Nucleoside—2′,3′/3′,5′-Bis(thio)phosphate Analogues Are Promising Antioxidants Acting Mainly via Cu^{+}/Fe^{2+} Ion Chelation

Bosmat Levi Hevroni, Alon Haim Sayer, Eliav Blum, and Bilha Fischer*

Department of Chemistry, Bar Ilan University, Ramat-Gan 52900, Israel

Supporting Information

ABSTRACT: We synthesized a series of adenine/guanine 2′,3′- or 3′,5′-bisphosphate and -bisphosphorothioate analogues, **1**−**6**, as potential Cu^{+}/Fe^{2+} chelators, with a view to apply them as biocompatible and water-soluble antioxidants. We found that electron paramagnetic resonance (EPR)-monitored inhibition of OH radicals production from H_2O_2, in an Fe^{2+}-H_2O_2 system, by bisphosphate derivatives **1**, **3**, and **5** (IC_{50} = 36, 24, and 40 μM, respectively), was more effective than it was by ethylenediaminetetraacetic acid (EDTA), by a factor of 1.5, 2, and 1.4, respectively. Moreover, 2′-deoxyadenosine-3′,5′-bisphosphate, **1**, was 1.8- and 4.7-times more potent than adenosine 5′-monophosphate (AMP) and adenosine 5′-diphosphate (ADP), respectively. The bisphosphorothioate derivatives **2**, **4**, and **6** (IC_{50} = 92, 50, and 80 μM, respectively), exhibited a dual antioxidant activity, acting as both metal-ion chelators and radical scavengers [2,2′-azino-bis(3-ethylbenzothiazoline-6-sulphonic acid) (ABTS) assay data indicates IC_{50} = 50, 70, and 108 μM vs 27 μM for Trolox]. Only 2′-deoxyadenosine-3′,5′-bisphosphorothioate, **2**, exhibited good inhibition of Cu^{+}-induced H_2O_2 decomposition (IC_{50} = 78 vs 224 μM for EDTA). Nucleoside−bisphosphorothioate analogues (**2**, **4**, and **6**) were weaker inhibitors than the corresponding bisphosphate analogues (**1**, **3**, and **5**), due to intramolecular oxidation under Fenton reaction conditions. ^{1}H- and ^{31}P NMR monitored Cu^{+} titration of **2**, showed that Cu^{+} was coordinated by both 3′,5′-bisphosphorothioate groups, as well as N7-nitrogen atom, while adenosine-2′,3′-bisphosphorothioate, **6**, coordinated Cu^{+} only by 2′,3′-bisphosphorothioate groups. In conclusion, an additional terminal phosphate group on AMP/guanosine 5′-monophosphate (GMP) resulted in Fe^{2+}-selective chelators highly potent as Fenton reaction inhibitors.

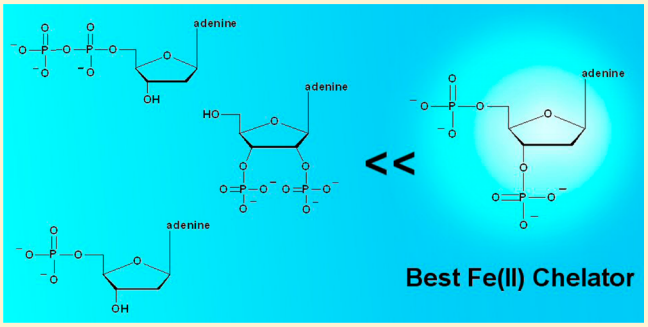

1. INTRODUCTION

Oxidative stress is caused when there is a disturbance in the pro-oxidants−antioxidant balance in favor of the former leading to potential damages.[1] The main species involved in the oxidative damage are reactive oxygen species (ROS), formed in several physiological processes, including the electron-transport chain in the mitochondria, auto-oxidation of some neurotransmitters, and during hypoxia or ischemia. Oxidative stress damages are associated with various diseases, including Alzheimer's disease,[2] amyotrophic lateral sclerosis (ALS),[3] Parkinson's disease, diabetes,[4] ischemia/reperfusion neuronal injuries, human cancers, as well as the aging process itself.

Reactive oxygen species include superoxide radical, O_2^{-}, hydroxyl radical, $HO^{\bullet}$, hydroperoxyl radical, $HOO^{\bullet}$, hydrogen peroxide, H_2O_2, singlet oxygen, $^{1}O_2$, and ozone, O_3. ROS such as $HO^{\bullet}$ and $HOO^{\bullet}$ are highly reactive. Harmful OH radicals attack any component in living organisms, including proteins, DNA, and lipids, at the rate of 10^{9}−10^{10} M^{-1} s^{-1}.[5] These reactions between cellular components and radicals lead to DNA damage, mitochondrial malfunction, cell membrane damage, and eventually cell death.

Activation of oxygen to ROS is energy-dependent and requires an electron donation. In biological systems transition metal ions (Fe^{2+}, Cu^{+}) can act as electron donors. OH radicals are generated from the less-damaging ROS, superoxide radical anion and hydrogen peroxide, in a Fenton or Haber−Weiss reaction catalyzed by ferrous or cuprous ions. The quest for therapeutic agents targeting the removal of toxic OH radicals, either by radical scavenging or by metal ion chelation mechanisms, spans the last three decades. The need for Cu/Fe-chelators to inhibit oxidative damage resulted in the identification of compounds such as clioquinol,[6] verapamil,[7] desferroxamine,[8] and tridentate triazolyl.[9]

The lack of biocompatibility of many of the synthetic metal chelators triggered the search for naturally occurring metal chelators. A few of these chelators, for example, phytic acid,[10] proved to be promising antioxidants. However, most others, including tea catechins,[11] hydroxytyrosol,[12] and chlorophyll derivatives,[13] showed low antioxidant activity, and some of them even exhibited pro-oxidant properties.[14]

Purine nucleotide analogues containing both the phosphate chain and the purine ring nitrogen atoms (e.g., N7 or N1) are natural metal-ion chelators.[15−17] Recently, we have studied

Received: October 24, 2013
Published: January 10, 2014

   dx.doi.org/10.1021/ic402671q | Inorg. Chem. 2014, 53, 1594−1605

natural nucleotides and the corresponding phosphorothioate analogues, as well as inorganic phosphates, as biocompatible and water-soluble inhibitors of Fenton reaction. We found that certain natural and synthetic adenine (A) nucleotides at submillimolar concentrations can prevent OH radical production from H_2O_2 in the presence of Cu^+/Fe^{2+} ions better than standard antioxidants and, thus, can possibly prevent damage of oxidative stress.[17,18]

Later, we found that nucleotide analogues such as adenine-(guanine) 5′-triphosphate−γ-sulphonic acid (A(G)TP−γ-S) and adenine(guanine) 5′-diphosphate−β-sulphonic acid (A-(G)DP−β-S) are most effective antioxidants inhibiting ROS production in PC12 cells (a clonal pheochromocytoma cell line) under oxidizing conditions ($FeSO_4$). ATP−γ-S was found to be a highly effective antioxidant, with IC_{50} = 180 nM versus 20 μM for Trolox,[19] being >100-fold more potent than ATP in inhibiting ROS formation in PC12 cells under oxidative conditions.[19] Recently we found that these nucleotide analogues are also most effective neuroprotectants against Fe^{2+} oxidation.[20]

Previously, we noticed that terminal phosphorothioate groups improve metal-ion binding as compared to nonterminal phosphate groups (e.g., the ATP−γ-S-Zn^{2+} complex is more stable than the AP_3(β-S)A-Zn^{2+} complex by 1.5 log units).[21] In addition, a terminal phosphorothioate moiety enables better coordination of borderline metal ions such as Fe^{2+} as compared to that of a terminal phosphate.[17] Furthermore, a terminal phosphorothioate moiety significantly enhances metabolic stability[21] and ROS production in cells under oxidative stress, as compared to the parent nucleotide.[20]

Here, we report the synthesis of six A/G nucleoside−2′,3′/3′,5′-bis(thio)phosphate analogues (**1**−**6**, Figure 1) as potential

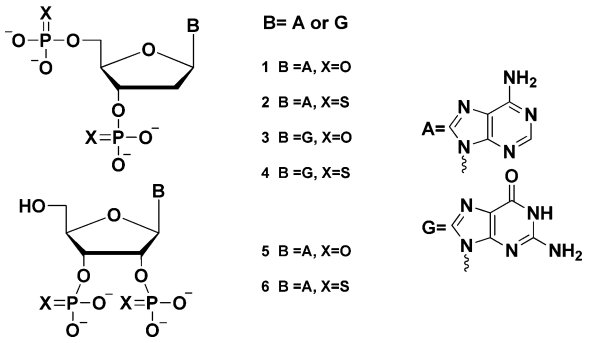

Figure 1. Nucleotide analogues **1**−**6**, studied here as potential antioxidants.

Fe^{2+}/Cu^+ chelators and the evaluation of these nucleosides as potential antioxidants. We evaluated derivatives **1**−**6** as Fenton reaction inhibitors by electron paramagnetic resonance (EPR) experiments, using 5,5′-dimethyl-1-pyrroline-*N*-oxide (DMPO) as a spin trap in Cu^+/Fe^{2+}-H_2O_2 solutions. To elucidate the mechanism of the Fenton reaction inhibition (i.e., metal-ion chelation and/or radical scavenging), we used metal-free systems and explored the inhibition of radical production by nucleoside−bisphosphate analogues by photolysis of H_2O_2, using EPR measurements, and by 2,2′-azino-bis(3-ethylbenzothiazoline-6-sulfonic acid) (ABTS) radical scavenging assay, using ultraviolet (UV) measurements. We studied the metal-ion selectivity and binding sites of analogues **1**−**6** by ^{1}H- and ^{31}P NMR-monitored Cu^+ titration and UV-monitored Fe^{2+}/Cu^+ titration.

2. RESULTS AND DISCUSSION

2.1. Synthesis. The synthesis of nucleoside−2′,3′-bis(thio)-phosphate and 3′,5′-bis(thio)phosphate analogues from nucleosides is especially challenging due to several difficulties: (i) Secondary alcohols, 2′- and 3′−OH, are far less reactive than 5′−OH.[22] (ii) 2′,3′-Vicinal diols in the ribonucleoside cause significant steric hindrance due to their close proximity. (iii) Intramolecular reactions may occur between the phosphorylating reagent and both neighboring hydroxyl groups to form undesirable side products (e.g., cyclic, di-, and triphosphates).[23] (iv) Unwanted reactions of the phosphorylating reagent may occur with reactive groups not only at the sugar but also the nucleobase (e.g., exocyclic amino group). Therefore, we attempted various synthetic pathways (**A**−**E**, Scheme 1) to obtain the desired modified nucleoside−bisphosphate analogues.

The analogue 2′-deoxyadenosine-3′,5′-bisphosphate (2′-dA3′5′PO, **1**), was prepared according to a previous procedure,[24] by treating 2′-deoxyadenosine with phosphoryl chloride and Proton Sponge (i.e., 1,8-bis(dimethylamino)-naphthalene) in trimethyl phosphate at 0 °C, in a one-pot reaction (pathway **A**).[24] This approach, however, was not as successful for the synthesis of analogue 2′-deoxyguanosine-3′,5′-bisphosphate (2′-dG3′5′PO, **3**), because of multiple side products and a complicated purification step. Alternatively, compound **3** was synthesized by pathway **B** according to literature.[25,26] Cyanoethyl phosphate pyridimium salt was reacted with an unprotected 2′-deoxyguanosine and dicyclohexylcarbodiimide (DCC) in dry pyridine for 3 d, followed by hydrolysis of the cyanoethyl group with LiOH to obtain 2′-dG3′5′PO, **3**.[25]

Thiophosphorylation of 2′-deoxynucleoside, to obtain 2′-deoxyadenosine-3′,5′-bisphosphrothioate (2′-dA3′5′PS, **2**), was carried out using the dioxaphospholane approach (pathway **C**), previously reported for the synthesis of either adenosine 3′- or 5′-thiophosphates.[27] Here, we applied this approach to obtain the 3′,5′-bisphosphorothioate product (Scheme 2). To obtain 2′-dA3′5′PS, **2**, thiophosphorylation reagent 2-chloro-2-thio-1,3,2-dioxaphospholane was first prepared from ethylene glycol and thiophosphoryl chloride.[27] Thiophosphorylation reagent 2-chloro-2-thio-1,3,2-dioxaphospholane was added to a solution of 2′-deoxyadenosine in tetrahydrofuran (THF) and dimethylformamide (DMF), which was treated with tBuMgCl in THF. Product **8** was treated with NaCN in dimethyl sulfoxide (DMSO) for 18 h to give product **9**, followed by the addition of NaOH in ethanol (EtOH) to obtain product **2**, in 6% yield, upon β-elimination of acrylonitrile. The product was characterized by ^{31}P NMR, showing typical singlets at 43.7 and 43.3 ppm (Scheme 2).[27]

Pathway **C** could not be applied to obtain the corresponding guanosine analogue, because of the reactive groups on its nucleobase. Therefore, we applied pathway **B**, to obtain the newly synthesized 2′-deoxyguanosine-3′,5′-bisphosphrothioate (2′-dG3′5′PS, **4**). The thiophosphorylation reagent *S*-2-cyanoethyl phosphorothioate, **11**, was first prepared from acrylonitrile and a solution of trisodium phosphorothioate in water, at 0 °C.[28] Thiophosphorylation of 2′-deoxyguanosine, **10**, with **11** and DCC in dry pyridine for 3 d, resulted in product **12**. The final product was obtained after the removal of the cyanoethyl protecting group with potassium *tert*-butoxide in the presence of ethyl mercaptane, as acrylonitrile scavenger, in THF to obtain product **4** in 6% yield after LC (Scheme 3).

dx.doi.org/10.1021/ic402671q | Inorg. Chem. 2014, 53, 1594−1605

Scheme 1. Synthetic Pathways Attempted to Obtain Nucleotide Analogues 1−6

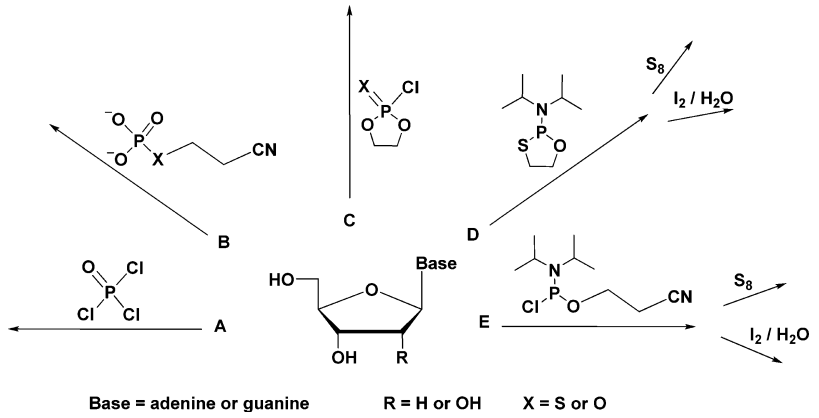

Scheme 2. Synthesis of 2′-dA3′5′PS, 2, via Pathway C[1]

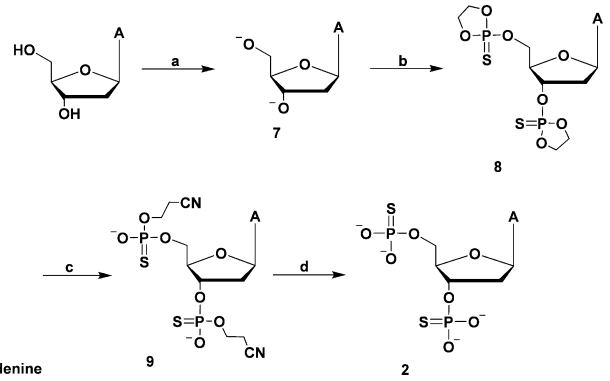

[1]Reagents and conditions: (a) tBuMgCl, dry THF, RT, 0.5 h. (b) 2-chloro-2-thio-1,3,2-dioxaphospholane, dry benzene, RT, 2.5 h. (c) NaCN, DMSO, RT, 18 h. (d) 0.23 M NaOH in EtOH, 2 h.

Product **4** was characterized by ^{31}P NMR, showing two typical signals at 43.71 and 43.27 ppm.

Because of the relatively low reactivity and the close proximity of the 2′ and 3′ hydroxyl groups, the synthesis of nucleoside−2′,3′-bisphosphorothioate derivatives was more complicated than that of the corresponding 3′,5′-analogues. After unsuccessfully applying method **B** (obtaining monophosphates as the main products) and having a limited success with method **C** (obtaining the bisphosphorothioate product **6,** but not the bisphosphate product **5**), other synthetic methods were implemented, using a more reactive trivalent phosphite instead of the phosphate reagent (methods **D** and **E**). The oxathiaphospholane approach, pathway **D**,[29] involved first the reaction of the thiophosphorylation reagent 2-*N*,*N*-diisopropylamino-1,3,2-oxathiaphospholane[29] with a N^6-benzoyladenosine, 5′-dimethoxytrityl (5′-DMT)-protected nucleoside, in the presence of tetrazole in dry CH_3CN, followed by sulfurization with elemental sulfur to obtain the bisphosphorothioate product **6**, or by oxidation with iodine/H_2O to obtain the bisphosphate product **5**. Pathway **D** resulted in low yields of the products and a complicated purification step, obtaining mainly the monophosphate product.

Methods **C** and **E** were more promising; pathway **C** led to the new compound adenosine-2′3′-bisphosphorothioate (A2′3′PS, **6**), in 18% yield, and pathway **E**, phosphoramidite methodology, gave the previously reported adenosine-2′3′-bisphosphate (A2′3′PO, **5**),[30] in 17% yield (Scheme 4). Specifically, the newly synthesized A2′3′PS, **6**, was prepared from 5'-tertybutyldimethylsilyladenosine (5′-TBDMS-A),[31] treated first with tBuMgCl in THF, followed by phosphorylation with 2-chloro-2-thio-1,3,2-dioxaphospholane in THF. Intermediate adenosine-bis(2-thio-1,3,2-dioxaphospholane) was then treated by CN^- in DMSO for 18 h, followed by addition of 0.23 M NaOH in EtOH. Finally, the 5′-TBDMS group was removed by tetra-*N*-butylammonium fluoride (TBAF) to obtain A2′3′PS, **6** (18% yield after LC).[27] The product was characterized by ^{31}P NMR, showing two typical signals at 51.24 and 49.64 ppm.

The product A2′3′PO, **5**, was prepared from N^6-benzoyl 5′-DMT-protected adenosine, treated with a trivalent phosphoramidite reagent and then oxidized with iodine. Specifically, compound **13** was treated with 2-cyanoethyl *N*,*N*-diisopropylchlorophosphoramidite and dry *N*,*N*-diisopropylethylamine at −80 °C in dry THF, to obtain compound **14**. Subsequently 3-hydroxypropionitrile was added, followed by the addition of tetrazole in dry acetonitrile, to give compound **15**. An oxidation

Scheme 3. Synthesis of 2′-dG3′5′PS, 4, via Pathway B[2]

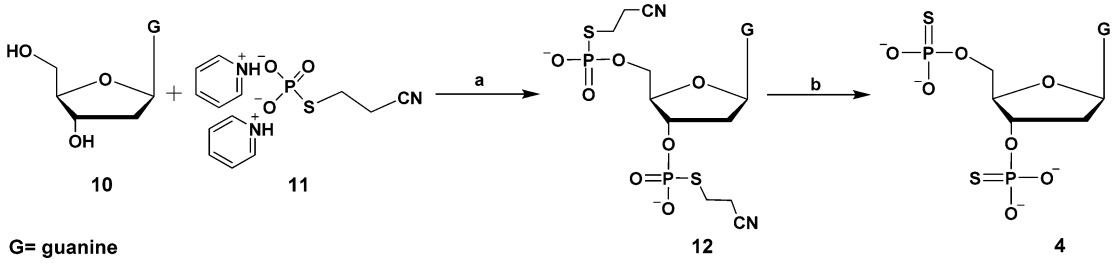

[2]Reagents and conditions: (a) 19.2 equiv of DCC, dry pyridine, RT, 3 d. (b) Potassium *tert*-butoxide, EtSH, THF, 2 h, RT.

dx.doi.org/10.1021/ic402671q | *Inorg. Chem.* 2014, 53, 1594−1605

Scheme 4. Synthesis of A2′3′PO, 5, via Pathway E[3]

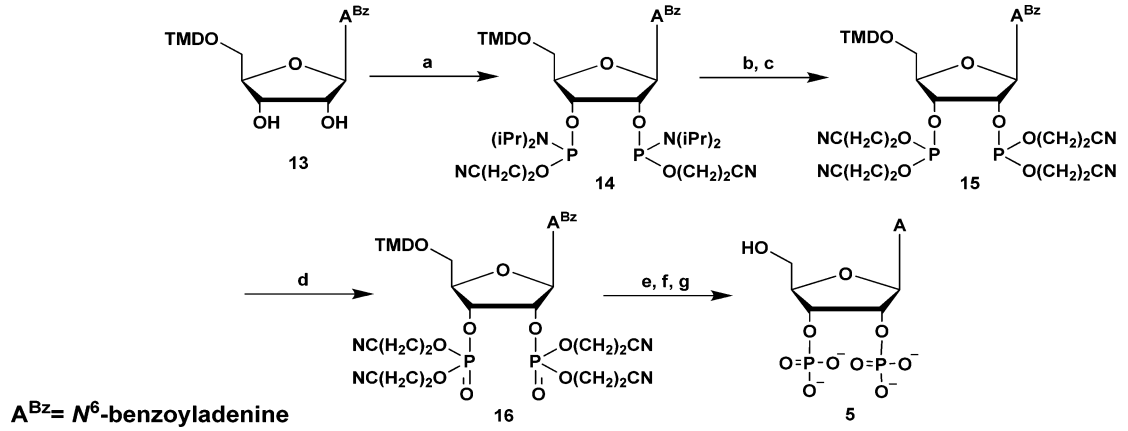

[3]Reagents and conditions: (a) 2-cyanoethyl *N,N*-diisopropylchlorophosphoramidite, *N,N*-diisopropylethylamine, dry THF, −80 °C, 2 h. (b) 3-Hydroxypropionitrile, 0.5 h. (c) Tetrazole, dry CH_3CN, 16 h. (d) I_2 in THF/pyridine/H_2O (7:2:1 v/v/v), −80 °C to RT, 15 min. (e) Potassium *tert*-butoxide, THF, 5 h, RT. (f) 80% AcOH, 2 h, RT. (g) ∼24% NH_4OH, 50 °C, overnight.

step was then performed, yielding compound **16**, followed by three subsequent deprotection steps to obtain the desired product **5** in 17% yield, after LC (Scheme 4).[30] The product was characterized by ^{31}P NMR, showing two typical signals at −0.18 and 0.39 ppm.

2.1.1. Nucleoside-2′,3′- and 3′,5′-bisphosphate Analogues Are Highly Active Antioxidants, Preferring Fe^{2+} over Cu^{+} Chelation. **2.2. Evaluation of the Antioxidant Effect of Compounds 1−6.** The modulation of OH radicals formation from H_2O_2 in the Fe^{2+}/Cu^{+}-induced Fenton reaction by compounds **1**−**6** was monitored by EPR. As the hydroxyl radical formed in the reaction is extremely short-lived, we used DMPO as a spin trap.[32] DMPO−OH adduct was then detected by EPR. The addition of chelators to the Fe^{2+}/Cu^{+}-H_2O_2 mixture lowers the DMPO−OH signal due to metal-ion chelation and/or radical scavenging (Figure 2).[17] The inhibition of radical production by compounds **1**−**6** (expressed in IC_{50} values, Table 1) was compared to the inhibitory effect of a metal-ion chelator, ethylenediaminetetraacetic acid (EDTA), and to the OH radical scavenging activity of the potent antioxidant Trolox (i.e., 6-hydroxy-2,5,7,8-tetramethylchroman-2-carboxylic acid). In addition we compared the antioxidant activity of compounds **1**−**6** to related natural nucleotides such as 2′-deoxyadenosine-5′-monophosphate (5′-dAMP), 2′-deoxyguanosine-5′-monophosphate (5′-dGMP), adenosine-3′-monophosphate (3′-AMP), and adenosine-5′-diphosphate (ADP).

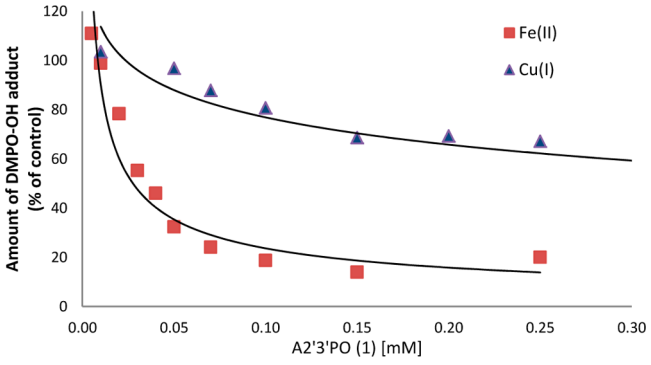

Figure 2. Modulation of Fe^{2+}- and Cu^{+}-induced Fenton reaction by A2′3′PO, **5**. Reactions were performed in 1 mM Tris buffer, containing 0.1 mM $FeSO_4$ or $Cu(CH_3CN)_4PF_6$, 10 mM H_2O_2, 10 mM DMPO pH 7.04, and 0−4 mM ligand. The amount of DMPO−OH adduct is given as percentage of control, which contains only metal, H_2O_2, and DMPO.

Table 1. Activity of Derivatives 1−6 and Selected References as Inhibitors of OH Radicals Formation in Cu^{+}/Fe^{2+}−H_2O_2 Solution[a]

		IC_{50} (μM)	
no.	compound	Fe^{2+}-H_2O_2	Cu^{+}-H_2O_2
1	2′-dA3′5′PO	36 ± 2	354 ± 19
2	2′-dA3′5′PS	92 ± 1	78 ± 4
3	2′-dG3′5′PO	24 ± 0	361 ± 11
4	2′-dG3′5′PS	50 ± 4	290 ± 11
5	A2′3′PO	40 ± 2	NA[b]
6	A2′3′PS	80 ± 3	NA
7	EDTA	56 ± 3	224 ± 10
8	Trolox	56 ± 1	NA
9	5′-dAMP	63 ± 1	NA
10	5′-dGMP	66 ± 1	NA
11	3′-AMP	111 ± 5	NA
12	ADP	170 ± 6	332 ± 2

[a]IC_{50} values represent the compound's concentration that inhibits 50% of the OH radical amount produced in the control reaction. [b]NA, not available. The minimal amount of radical production exceeds 50%.

The chelation of the metal ions Fe^{2+} and Cu^{+} by derivatives **1**−**6** depends on the hard−soft acid−base nature of both metal-ion and nucleotide chelators. Therefore, we expected bisphosphate derivatives **1**, **3**, and **5** to chelate borderline ferrous ions better than soft cuprous ions and the bisphosphorothioate derivatives **2**, **4**, and **6** to chelate soft cuprous ions better than ferrous ions. We found that in the Fe^{2+}-H_2O_2 system, both 2′-dA3′5′PO and 2′-dG3′5′PO, analogues **1** and **3**, were more potent antioxidants (IC_{50} 36 and 24 μM, respectively) than EDTA by a factor of 1.5 and 2, respectively. In addition, compound **1**, bearing two terminal phosphate moieties, was 1.8 and 4.7 times more potent than 5′-AMP and ADP, respectively, supporting our assumption that two terminal phosphate moieties enhance Fe^{2+} chelation versus one terminal and one nonterminal phosphate moiety. Moreover, the position of the

dx.doi.org/10.1021/ic402671q | Inorg. Chem. 2014, 53, 1594−1605

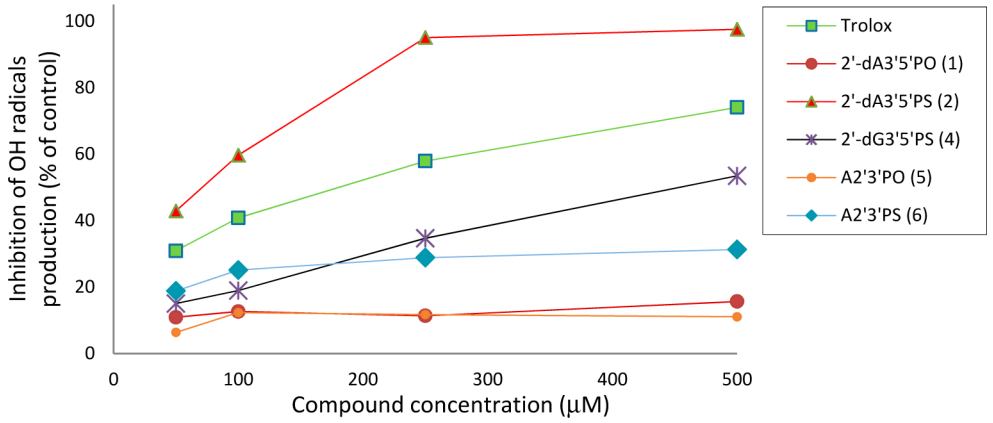

Figure 3. Evaluation of radical scavenging by selected derivatives (**1**, **2**, and **4**–**6**), using EPR technique. The inhibition of OH radical production by photolysis of H_2O_2 is presented as a percent of control.

terminal phosphate also affects chelation, as demonstrated by comparing 3′-AMP to 5′-AMP (IC_{50} values of 111 and 63 μM, respectively). When the terminal phosphate is located at the 5′ position, it is closer to the purine ring, specifically, to the N7 position. The close proximity of these two metal binding sites could rationalize the lower IC_{50} value of 5′-AMP versus 3′-AMP.

Surprisingly, the adenosine bisphosphorothioate derivatives **2** and **6** had a similar IC_{50} value (92 and 80 μM, respectively), which means that the position of the thiophosphate groups (i.e., 2′,3′- vs 3′,5′-) had no substantial effect on Fe^{2+} chelation. These observations may be explained by the rapid oxidation of phosphorothioate compounds to form the corresponding disulfide dimers under Fenton reaction conditions,[17] which may reduce the chelating ability of this derivative. The guanosine bisphosphorothioate derivative, **4**, had a similar IC_{50} value to that of EDTA (50 vs 56 μM).

In general, as expected for the Cu^{+}-H_2O_2 system, we obtained higher IC_{50} values for the bisphosphate analogues. The hard bisphosphate ligands do not efficiently chelate the soft cuprous metal ions (**1** and **3**, IC_{50} 354 and 361 μM, respectively), unlike their selectivity toward the borderline Fe^{2+}-ion. Moreover, the position of the phosphate groups (i.e., 2′,3′- vs 3′,5′-) had an effect on Cu^{+} chelation. The IC_{50} value for derivatives **5** and **6** could not be determined up to 500 μM, thus indicating that vicinal (thio)phosphate groups are far less capable of Cu^{+} chelation. Apparently, the distance of 2′,3′-bisphosphate groups from the purine N7 chelating site reduces the chelating ability of analogues **5** and **6**. In the Cu^{+}-H_2O_2 system, we observed a more complicated behavior of nucleoside–bisphosphorothioate analogues than that in the Fe^{2+}-H_2O_2 system. While analogue 2′-dA3′5′-PS, **2**, had an IC_{50} value of 78 μM (vs 224 μM for EDTA), in the case of the analogue A2′3′PS, **6**, the IC_{50} value could not be obtained up to 500 μM. The same behavior was observed for its bisphosphate analogue, **5**, as explained above. The analogue 2′-dG3′5′-PS, **4**, exhibited a higher IC_{50} value than 2′-dA3′5′-PS, **2** (290 vs 78 μM). These surprising findings were elucidated by exploring the radical scavenging properties of analogues **1**–**6**, as described below.

2.3. Nucleoside-2′,3′- and 3′,5′-Bisphosphate Analogues Are Not Radical Scavengers, While 2′,3′- and 3′,5′-Bisphosphorothioates Are Mediocre to Good Radical Scavengers. Since the Fenton reaction can be inhibited by both metal-ion chelators and radical scavengers, we also evaluated analogues **1**–**6** and selected references as radical scavengers, using two complementary methods. First, we produced OH radicals by photolysis of H_2O_2[33,34] and monitored radical scavenging by analogues **1**–**6** using EPR. Second, we added these analogues to ABTS radical cation ($ABTS^{\bullet+}$) and monitored radical scavenging by UV measurements (ABTS decolorization assay).[35]

*2.3.1. Modulation of Concentration of OH Radicals Obtained by Photolysis of H_2O_2 by Analogues **1**, **2**, and **4**–**6**.* The radical scavenging activity of nucleotide analogues **1**, **2**, and **4**–**6** was determined as a function of the antioxidant concentration and was calculated relative to a control measurement, which is the maximal production of OH radicals via photolysis of H_2O_2, in the absence of a radical scavenger. The experiment conditions (e.g., DMPO and H_2O_2 concentrations) were similar to those of the metal-ion-catalyzed Fenton reaction. We evaluated the radical scavenging by the selected derivatives at four concentrations (50, 100, 250, and 500 μM, Figure 3). To analyze the data and compare the radical scavenging capacity of the compounds, we focus on their activity at a single concentration-point, 250 μM. As we expected, compounds **1** and **5**, bearing phosphate moieties, did not present any significant scavenging property, only 10% inhibition of OH radicals formation by radical scavenging. Namely, their antioxidant activity in a Fenton system was due mainly to their activity as metal-ion chelators.

We found that analogues bearing a thiophosphate moiety, such as compounds **2** (2′-dA3′5′PS) and **4** (2′-dG3′5′PS), displayed radical scavenging activity (95% and 35% inhibition of OH radicals formation, for **2** and **4**, respectively, vs 58% for Trolox; see Figure 3) in addition to their above-mentioned metal-chelating activity.

Furthermore, the position of the thiophosphate groups (i.e., 2′,3′- vs 3′,5′-) affects the antioxidant activity of the related nucleoside analogues. While 2′-dA3′5′PS, **2**, presented a good scavenging capacity, A2′3′PS, **6**, presented only mild scavenging activity (95% vs 29% inhibition of OH radicals formation for **2** and **6**, respectively). Compounds **2** and **6** scavenge radicals by contributing electrons to OH radicals, thus forming a 3′,5′- or 2′,3′-disulfide bond (e.g, 2′-S–S-3′), respectively. We hypothesize that the reason for compound **2** being a better antioxidant than **6** may be related to the presence of a 5′-thiophosphate, namely, a less hindered and therefore more reactive group. (This hypothesis is further supported by

dx.doi.org/10.1021/ic402671q | Inorg. Chem. 2014, 53, 1594–1605

the reaction of compounds **2** and **6** in H_2O_2 with Ellman's reagent, see below.)

2.3.2. Evaluation of Radical Scavenging Activity of Analogues 1−6 Using ABTS Radical Cation Assay. Next, we evaluated the antioxidant activity of analogues **1**−**6** that is due to radical scavenging, using the ABTS decolorization assay.[35] $ABTS^{\bullet+}$, formed by the oxidation of 2,2′-azino-bis-(3-ethylbenzthiazoline-6-sulfonic acid, ABTS, with potassium persulfate, absorbs light at 645, 734, and 815 nm. The scavenging of the $ABTS^{\bullet+}$ radical by analogues **1**−**6** was determined as a function of the antioxidant concentration and calculated relative to the reactivity of Trolox as a standard antioxidant (Table 2).

Table 2. Scavenging of $ABTS^{\bullet+}$ by Selected Nucleoside−Bisphosphorothioate Analogues vs Trolox

compound	IC_{50} (μM)
2′-dA3′5′PS (**2**)	51 ± 3
2′-dG3′5′PS (**4**)	70 ± 1
A2′3′PS (**6**)	108 ± 6
Trolox	27 ± 1

We found that analogues **1**, **3**, and **5** and reference compounds 5′-dAMP, 5′-dGMP, and 3′-AMP did not show any significant activity as radical scavengers (IC_{50} > 100 μM). However, analogues **2**, **4**, and **6**, bearing a thiophosphate moiety, presented mild radical scavenging activity (IC_{50} of 51, 70, and 108 μM, respectively, as compared to IC_{50} of 27 μM for Trolox). Here, again, we observed the effect of the position of the thiophosphate groups (i.e., 2′,3′- vs 3′,5′-) on the scavenging capacity of a nucleoside−bisphosphorothioate analogue, making 2′-dA3′5′PS, **2**, 1.4-fold more active than A2′3′PS, **6**. These results correlate with the above findings for the inhibition of OH radical formation by photolysis of H_2O_2.

2.4. Nucleoside Bisphosphorothioate Analogues under Fenton Reaction Conditions Undergo Intramolecular Oxidation. To characterize the actual nucleoside−bisphosphorothioate antioxidant species formed under Fenton reaction conditions, we have monitored the oxidation of analogues 2′-dA3′5′PS, **2**, and A2′3′PS, **6**, in the presence of Ellman's reagent, **17** (5,5′-dithiobis(2-nitrobenzoic acid), DTNB),[36,37] to the corresponding disulfides, **19** and **20**, respectively, using UV measurements. Ellman's reagent, **17**, was used to detect and quantify the amount of free thiols present (Figure 4). Ellman's reagent rapidly forms a disulfide bond with thiophosphate in an aqueous solution and releases nitrobenzoic acid thiolate ion, **18**, showing maximal absorbance at 412 nm.

Compounds **2** or **6** were added to Ellman's reagent in aqueous solution; as a result, the absorbance of the nitrobenzoic acid thiolate ion appeared at 412 nm, indicating that compounds **2** and **6** had initially free phosphorothioate groups (Figure 5). When compounds **2** or **6** and Ellman's reagent were added to the Fenton reaction mixture (Fe^{2+}/H_2O_2), no absorbance appeared at 412 nm. These results indicate that under Fenton reaction conditions, the starting free phosphorothioate groups undergo oxidation to form an intramolecular disulfide ring, **19** or **20**, thus preventing the formation of **18**. We compared the kinetics of the rate of oxidation of compound **2** versus **6** in the presence of DTNB (**17**) and found that **2** was oxidized faster than **6** (Figure 5B). As mentioned above, we speculate that this result is due to the presence of a less hindered, and therefore more reactive, 5′-thiophosphate group. The loss of part of the nucleoside−bisphosphorothioate population due to intramolecular oxidation under Fenton reaction conditions explains why bisphosphorothioate analogues **2**, **4**, and **6** were weaker ion chelators and hence weaker inhibitors than the corresponding bisphosphate analogues **1**, **3**, and **5**.

2.5. Nucleoside-2′,3′-bisphosphorothioate Coordinates Cu^+ via Both Phosphorothioate Groups, While 3′,5′-Bisphosphorothioate Coordinates Cu^+ via Both Phosphorothioate Groups and N7. Interaction of nucleotides with metal ions depends on the hard−soft acid−base nature of both metal-ion and nucleotide chelator. First and second row metal ions interact solely with the phosphate part of the nucleotide[36,37] ("open" form complex), while transition metal ions can form macrochelates[38−40] by binding to both phosphate and base moieties[36,41,42] ("closed" form complex). Furthermore, there are at least two types of macrochelates of metal-ion (purine nucleotide) complexes: one in which the metal ion binds directly to N7 of the purine residue (innersphere coordination) and one in which metal-ion coordination involves a water molecule between N7 and a metal-ion (an outersphere interaction).[42] One of the sensitive methods to study the interaction of metal ion with nucleotides is by NMR measurements.[38,39,43]

To explore Cu^+ coordination by analogues **2** and **6** (2′,3′- vs 3′,5′-bisphosphorothioate analogues), we performed Cu^+ titrations monitored by ^1H- and ^{31}P NMR spectroscopy. NMR spectra indicating Cu^+ binding to analogues **2** and **6** are

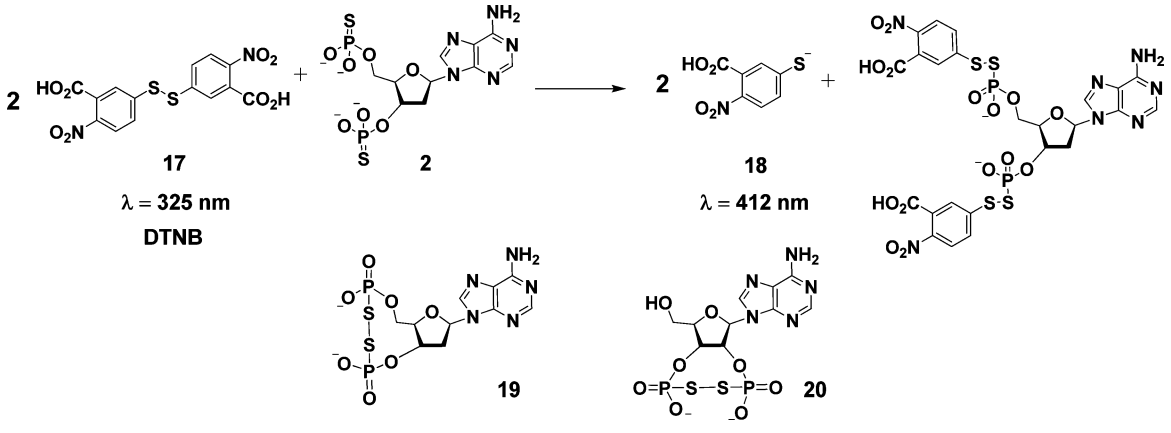

Figure 4. Reaction of Ellman's reagent with 2′-dA3′5′PS, **2**, in aqueous solution.

dx.doi.org/10.1021/ic402671q | Inorg. Chem. 2014, 53, 1594−1605

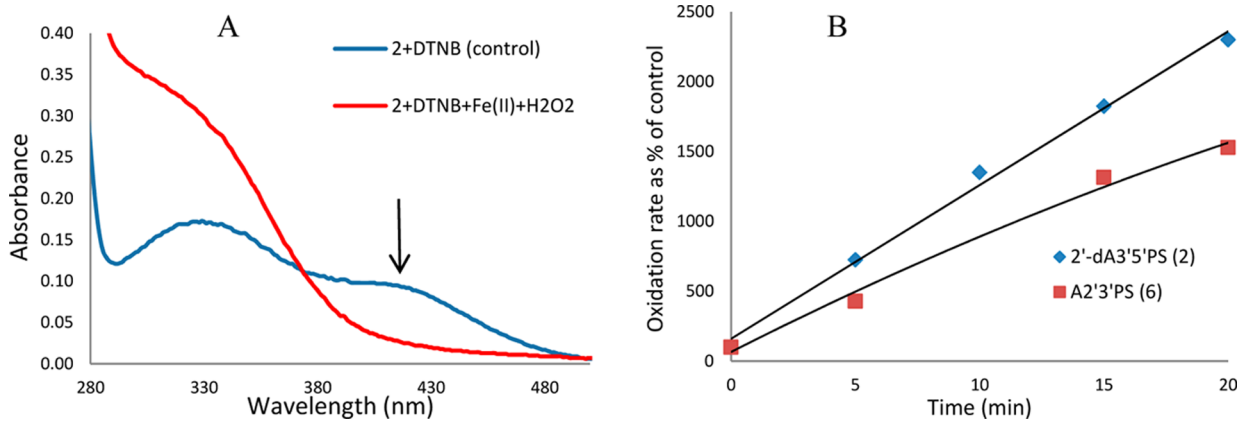

Figure 5. (A) Monitoring the oxidation of comopund **2** under Fenton reaction conditions. The experiment was performed in 1 mM Tris buffer (pH = 7.4), in the presence of 0.1 mM $(NH_4)_2Fe(SO_4)_2$, 10 mM H_2O_2, and 10 mM DTNB (red line). Control solutions contained 0.1 mM **2** and DTNB (blue line). Each graph represents the absorbance measured 20 min after DTNB addition. (B) Comparing the rate of oxidation of compounds **2** and **6** in the presence of DTNB.

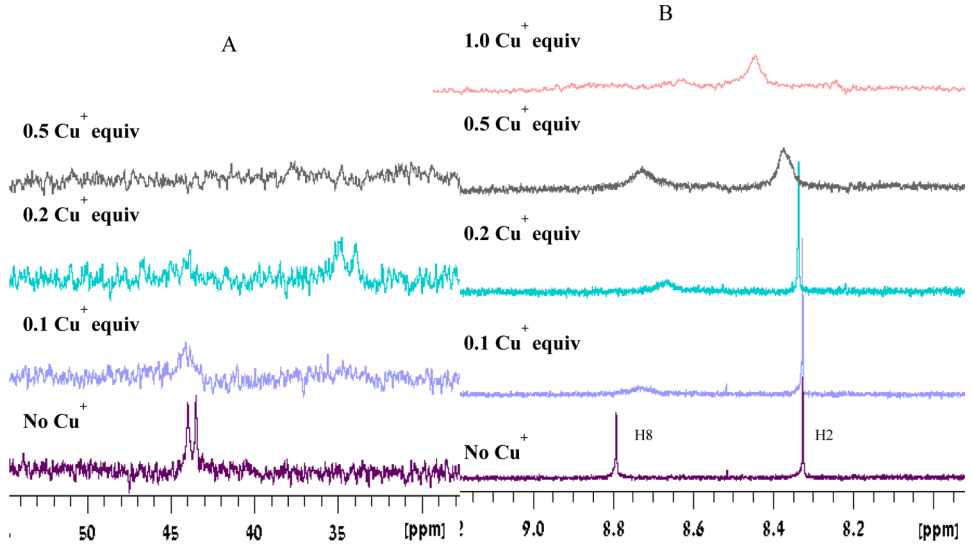

Figure 6. Titration of 2.8 mM **2** in D_2O at pD 7.4 with Cu^+. (A) ^{31}P NMR spectra were measured at 162 MHz, 300 K. (B) ^1H NMR spectrum was measured at 400 MHz, 300 K.

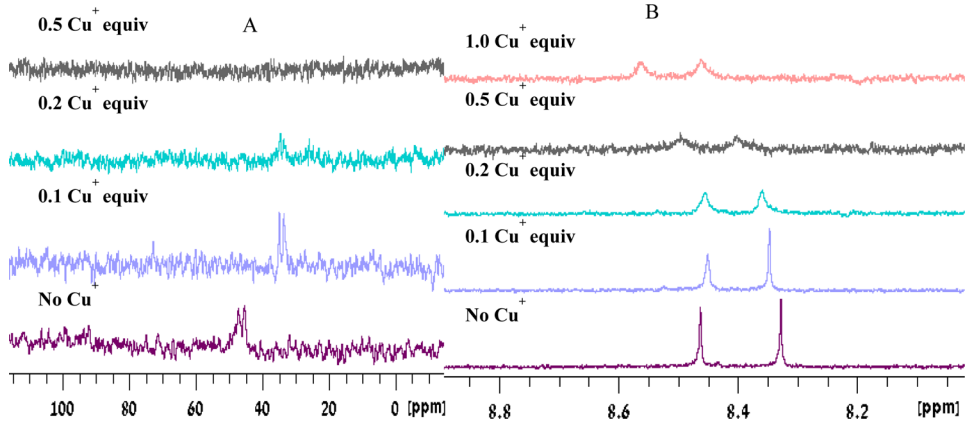

Figure 7. Titration of 2.6 mM **6** in D_2O at pD 7.2 with Cu^+. (A) ^{31}P NMR spectra were measured at 162 MHz, 300 K. (B) ^1H NMR spectrum was measured at 400 MHz, 300 K.

shown in Figures 6 and 7, respectively. The shift of NMR signals as well as their line broadening indicates Cu^+ coordination to several atoms in analogues **2** and **6**.

Solution of analogue **2** or **6** in D_2O (pD= 7.4, 5% CD_3CN) was titrated by $Cu(CH_3CN)_4PF_6$ in CD_3CN and monitored by ^1H- and ^{31}P NMR. A relatively low nucleotide concentration

dx.doi.org/10.1021/ic402671q | Inorg. Chem. 2014, 53, 1594−1605

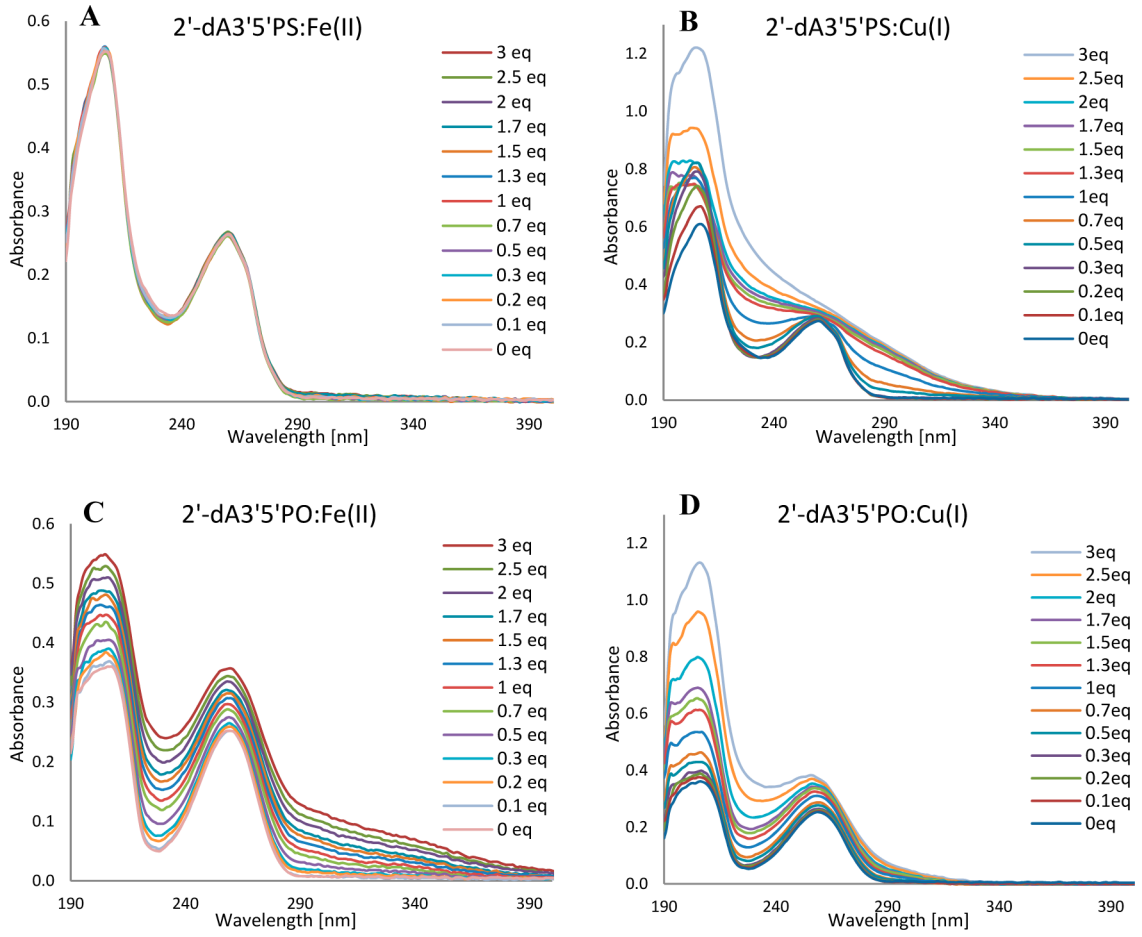

Figure 8. Titrations of compounds **1** and **2** with up to 3 equiv of Fe^{2+} or Cu^{+}, as monitored by UV−vis spectra. UV−vis spectra of (A) **2**-Fe^{2+}, (B) **2**-Cu^{+}, (C) **1**-Fe^{2+}, (D) **1**-Cu^{+}.

was used (ca. 3 mM) to avoid intermolecular base stacking (π-stacking interactions) in aqueous solutions.[44] Chemical shifts (δ_H, δ_p) were measured, at different Cu^{+} concentrations.

Addition of 0.1 equiv of Cu^{+} to compound **2** caused a line broadening in the ^{31}P NMR spectrum (Figure 6A), while addition of 0.2 equiv of Cu^{+} to compound **2** caused upfield shift of both P3′ and P5′ by 9.78 ppm in addition to line sharpening. The large shift of chemical shifts indicates that the thiophosphate moiety has a high affinity to Cu^{+} and that both thiophosphate groups are involved in metal-ion binding. Further addition of 0.5 equiv of Cu^{+} caused a massive line broadening, resulting from dynamic equilibrium between free **2** and the Cu^{+}-**2** complex.

^{1}H NMR-monitored Cu^{+} titration of compound **2** exhibited a line broadening and an upfield shift of H8 purine proton, upon the addition of 0.1 equiv of Cu^{+} (Figure 6B). The H8 signal was shifted upfield by 0.06 ppm, whereas the chemical shift of H2 did not change. The shift of the H8 signal implies that N7 is a coordination site of Cu^{+}. Upon the addition of 0.2 equiv of Cu^{+}, the H8 signal was further shifted by 0.05 ppm, and the H2 signal was insignificantly shifted ($\Delta\delta$ = 0.01); however, when 0.5 equiv of Cu^{+} was added, the H2 signal also broadened.

The titration was performed at pD = 7.4. Hence, the terminal thiophosphate was not protonated (pK_a < 5.0),[45] which means that the observed shift of chemical shift of the thiophosphate moiety was due to coordination with Cu^{+} and not acid−base equilibrium of the terminal thiophosphate. These NMR results showed that in the **2**-Cu^{+} complex, both thiophosphate groups (P3′ and P5′) as well as the N7 nitrogen atom are involved in Cu^{+} binding, probably in a closed form.

NMR spectra of monitored Cu^{+} titration of compound **6** showed similar features as those of the ^{31}P spectra of Cu^{+}-titrated **2**, but a different pattern was observed in the ^{1}H NMR spectra. Addition of 0.1 equiv of Cu^{+} to compound **6** caused a significant upfield shift of the bisphosphorothioates signals ($\Delta\delta$ = 11.88, Figure 7A) and caused a minor line sharpening. Upon addition of 0.2−0.5 equiv of Cu^{+}, line broadening was observed. As observed for compound **2**, the large shift upon addition of only 0.1 equiv of Cu^{+} to compound **6** indicates a high affinity of the thiophosphate moiety to Cu^{+} and that both thiophosphate groups are involved in chelation.

Upon addition of 0.1 equiv of Cu^{+} to compound **6** a minor downfield shift of the H2 signal ($\Delta\delta$ = 0.02) and a minor upfield shift of the H8 signal ($\Delta\delta$ = 0.01) was observed in the ^{1}H NMR spectrum (Figure 7B). Both signals exhibited line broadening upon addition of 0.2−0.5 equiv of Cu^{+}. These minor changes in the chemical shifts imply that N7/N3 nitrogen atoms are not involved in direct Cu^{+} binding, because of the relatively large distance of 2′ and 3′ positions to these nitrogen atoms, although they may be involved in an outersphere coordination of Cu^{+}. The downfield shift caused by the addition of 1 equiv of Cu^{+} may be because of a nonspecific effect.

2.6. Charge Transfer Band in UV Spectrum Indicates That Nucleoside−3′,5′-Bisphosphorothioate Coordi-

dx.doi.org/10.1021/ic402671q | Inorg. Chem. 2014, 53, 1594−1605

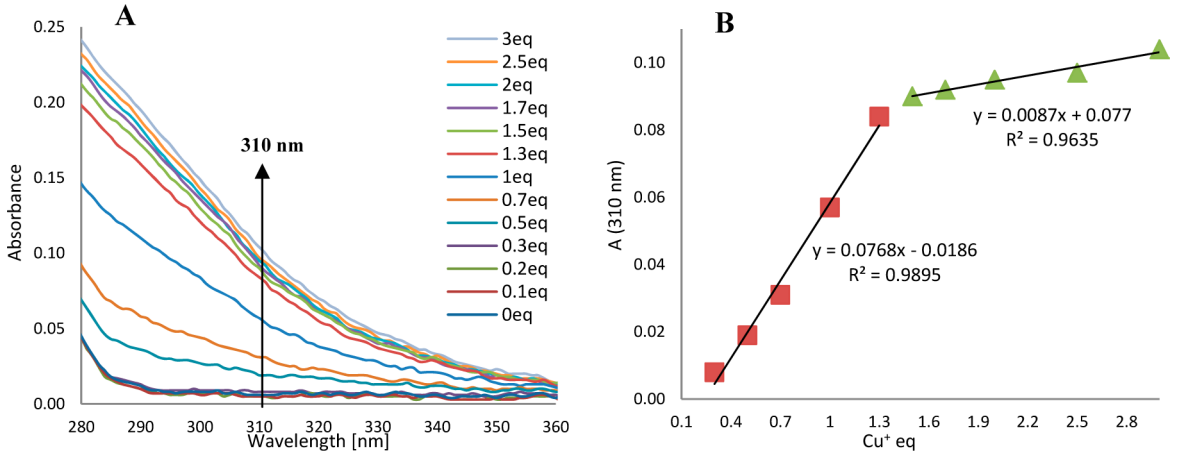

Figure 9. Titrations of compound **2** with Cu^+ as monitored by UV–vis spectra. (A) Charge-transfer band region in UV–vis spectra of the **2**-Cu^+ complex (0–3 equiv of Cu^+). (B) Cross section of UV–vis spectra at 310 nm.

nates Preferentially Cu^+, While Nucleoside–3′,5′-Bisphosphate Coordinates Preferentially Fe^{2+}. To study the interaction of nucleoside–bisphosphate analogues with metal ions, we also employed UV measurements of the complexes.[36,46] We performed Fe^{2+}/Cu^+ titrations of compounds 2′-dA3′5′PO, **1**, and 2′-dA3′5′PS, **2**, monitored by UV spectroscopy. Analogues **1** or **2** (0.02 mM), in 1 mM tris(hydroxymethyl)aminomethane (Tris) buffer (pH 7.4), were titrated with $Cu(CH_3CN)_4PF_6$ in CH_3CN or $FeSO_4$ in H_2O (2 mM). For each titration point, 1 μL of the metal-ion solution was added, and the absorbance was measured. One millimolar Tris buffer (pH 7.4) was measured as the blank.

The UV–vis spectra of the **1**- and **2**-Fe^{2+}/Cu^+ titrations are shown in Figure 8. At 0 equiv of metal ions, analogues **1** and **2** displayed absorbance of adenosine at 200 and 260 nm (Figure 8A–D).[47] Titrating analogue **2** with Fe^{2+} did not result in any visible change of the base absorbance (up to 3 equiv of Fe^{2+}, Figure 8A). Titration of **2** with Cu^+ resulted in a tail of charge-transfer band (300–330 nm) from the ligand-to-metal ion,[46] which increased upon the addition of Cu^+ (Figure 8B). These results correlate with the soft nature of the thiophosphate moieties of **2**, which prefer to coordinate the soft Cu^+ ion, rather than the borderline Fe^{2+} ion. Titration of **1** with Fe^{2+} and Cu^+ resulted in a tail of charge-transfer band in both cases, which is relatively small in the latter case (Figure 8C,D). These results correlate well with our EPR and NMR data for these compounds in the presence of Cu^+/Fe^{2+}.

We also estimated the metal-binding stoichiometry of compound **2** with Cu^+ (the only complex which reached saturation up to 3 equiv of metal ion addition), by UV–vis titration utilizing Yoe and Jones' method.[48] A cross-section analysis of the charge-transfer band region at 310 nm (Figure 9A) implied a 1:1.4 ligand:metal stoichiometry that probably corresponds to a 1:1 ratio (Figure 9B).

3. DISCUSSION AND CONCLUSIONS

Recently, we have identified natural nucleotides and the corresponding phosphorothioate analogues, as well as oligonucleotides and inorganic phosphates, as biocompatible and water-soluble inhibitors of Cu^+/Fe^{2+}-induced Fenton reaction.[17,18,21]

3.1. Nucleoside–2′,3′- and 3′,5′-bisphosphate Analogues Are Highly Active Antioxidants, Preferring Fe^{2+} over Cu^+ Chelation. Here, we proved that naturally occurring and synthetic A/G 2′,3′- or 3′,5′-bisphosphate and -bisphosphorothioate analogues, **1**–**6**, are also Cu^+/Fe^{2+} chelators that are potentially useful as biocompatible and water-soluble antioxidants. Specifically, we found that nucleoside–2′,3′- and 3′,5′-bisphosphate analogues are highly active antioxidants preferring chelation of Fe^{2+} over Cu^+. Furthermore, we found that terminal phosphate groups improve metal-ion binding as compared to nonterminal phosphate groups. Compound **1**, bearing two terminal phosphate moieties, was 1.8 and 4.7 times more potent than 5′-dAMP and ADP, respectively. Furthermore, bisphosphate derivatives **1**, **3**, and **5** in a Fe^{2+}-H_2O_2 system were more potent antioxidants than EDTA by a factor of 1.5, 2, and 1.4, respectively. The position of the phosphate groups in mononucleotides, for example, 3′- versus 5′-dAMP, did affect the chelation ability of Fe^{2+}, and 5′-dAMP was 1.8-fold more potent than 3′-AMP.

In general, bisphosphate analogues (**1**, **3**, and **5**) in the Cu^+-H_2O_2 system proved to be up to 12-fold less effective antioxidants than they were in the Fe^{2+}-H_2O_2 system. The "hard" bisphosphates ligands do not chelate the "soft" cuprous metal ions as efficiently as they chelate Fe^{2+}. Moreover, the position of the phosphate groups (i.e., 2′,3′- vs 3′,5′-) had an effect on the Cu^+ chelation. Specifically, derivative **5** proved to be an extremely poor Cu^+-induced Fenton reaction inhibitor versus 3′,5′-bisphosphate analogues. This phenomenon is possibly due to the relatively large distance of the 2′,3′-bisphosphate moieties from the purine N7-chelating site, forcing Cu^+-ion chelation only via the phosphate groups.

3.2. Nucleosides–2′,3′- and 3′,5′-bisphosphorothioate Exhibited a Dual Antioxidant Activity, Acting Both As Metal Ion Chelators and As Radical Scavengers. Bisphosphorothioate derivatives **2** and **6** exhibited a similar IC_{50} value in the Fe^{2+}-H_2O_2 system, which means that the position of the thiophosphate groups (i.e., 2′,3′- vs 3′,5′-) had no substantial effect on Fe^{2+} chelation. In the Cu^+-H_2O_2 system, however, while 2′-dA3′5′-PS, **2**, had an IC_{50} value of 78 μM (vs 224 μM for EDTA), in the case of A2′3′PS, **6**, the IC_{50} value could not be observed up to 500 μM. The guanosine homologue of compound **2** (2′-dG3′5′-PS, **4**) exhibited a higher IC_{50} value (290 μM) than that of **2** in Cu^+-H_2O_2 system, probably because the G nucleobase has a "harder" character than A.[49] Nucleoside–bisphosphorothioate analogues (**2**, **4**, and **6**) were weaker inhibitors than the corresponding

dx.doi.org/10.1021/ic402671q | Inorg. Chem. 2014, 53, 1594–1605

bisphosphate analogues (**1**, **3**, and **5**) because of their intramolecular oxidation under Fenton reaction conditions.

To evaluate the mechanism(s) of antioxidant activity of analogues **2**, **4**, and **6**, we explored the inhibition of radical production in a metal-free system and found that analogues bearing a phosphorothioate moiety, such as compounds **2** (2′-dA3′5′PS) and **4** (2′-dG3′5′PS), displayed radical scavenging activity in addition to their metal-chelating activity. Furthermore, the position of the thiophosphate groups (i.e., 2′,3′- vs 3′,5′-) affected the scavenging activity of the nucleoside−bisphosphorothioate analogues. While 2′-dA3′5′PS, **2**, presented a good scavenging capacity, A2′3′PS, **6**, presented mild radical scavenging activity. This phenomenon is due to the presence of a less-hindered, and therefore more-reactive, 5′-thiophosphate group. 3′,5′-Bisphosphate analogues **1**, **3**, and **5** did not present any significant radical scavenging ability, and their inhibitory activity is mainly due to metal-ion chelation.

The NMR-monitored Cu^+ titration data showed that in analogue **2**-Cu^+ complex, both thiophosphate groups (P3′ and P5′) as well as the N7 nitrogen atom are involved in Cu^+ binding, probably in a closed form. However, in analogue **6**-Cu^+ complex, the thiophosphate groups (P2′ and P3′) are most likely involved in Cu^+ binding through an open form. UV-monitored Fe^{2+}/Cu^+ titration further supported the metal-ion selectivity of bisphosphate versus bisphosphorothioate analogues in an aqueous solution. Specifically, analogue **1**, 2′-dA3′5′PO, coordinated preferentially Fe^{2+} ion rather than Cu^+ ion, while analogue **2**, 2′-dA3′5′PS, coordinated preferentially the soft Cu^+ metal ion.

In conclusion, an additional terminal (thio)phosphate group on an AMP/GMP scaffold resulted in increased Fe^{2+}/Cu^+ chelation. The bisphosphate derivatives **1** and **3** are potent antioxidants, acting mainly as Fe^{2+} chelators, being 1.5- and 2.3-fold more active than EDTA, respectively, and 1.8- and 2.8-fold more active than 5′-AMP and 5′-GMP, respectively. Derivatives **1** and **3** were 9.8- and 15-fold more selective for Fe^{2+} versus Cu^+. However, the bisphosphorothioate derivatives (**2**, **4**, and **6**) exhibited a dual antioxidant activity, acting as both metal-ion chelators and radical scavengers, where the 3′,5′-bisphosphorothioate analogues were found to be better radical scavengers than 2′,3′-bisphosphorothioate.

4. EXPERIMENTAL SECTION

4.1. General Information. Compounds **1**,[24] **2**,[27] **3**,[25] and **5**[30] were synthesized as reported before (see also Supporting Information). All air- and moisture-sensitive reactions were carried out in flame-dried, argon-flushed, two-neck flasks sealed with rubber septa, and the reagents were introduced with a syringe. All commercial reagents were used without further purification, unless otherwise noted. All reactants in moisture-sensitive reactions were dried overnight in a vacuum oven. The progress of the reactions was monitored by thin-layer chromatography on precoated Merck silica gel plates (60F-254). Visualization was accomplished by UV light. Absorption data were measured with a Shimadzu UV-2401PC ultraviolet−visible (UV−Vis) recording spectrophotometer. Preliminary purification of the synthesized compounds was performed by a liquid chromatography (LC) system (Isco UA-6) using a Sephadex DEAE-A 25 column, which was swelled in 1 M $NaHCO_3$ in the cold for 1 d. The resin was washed with high performance liquid chromatography (HPLC)-grade water before use until no UV absorption was detected. Separation was monitored by UV spectroscopy, with detection at 280 nm. Flash chromatography was carried out on silica gel (Davisil Art. 1000101501). Neutral compounds were separated on HPFC automated flash purification system (Biotage SP1 separation system (RP)). Final purification was achieved with an HPLC system (Merck-Hitachi), using a semipreparative reverse-phase column (Gemini 5 μm, C18 110 Å, 250 × 10.00 mm, Phenomenex, Torrance, USA). The ^1H NMR and ^{31}P NMR spectra were measured with Bruker AC-200 and AV-400 (200 and 400 MHz for ^1H NMR, 80.3 and 162 MHz for ^{31}P, respectively), or DMX-600 (600, 243, and 151 MHz for ^1H, ^{31}P, and ^{13}C, respectively) spectrometers. All spectra were measured at room temperature (RT) in D_2O samples, and chemical shifts were determined relative to HOD (4.79 ppm) as an internal standard for ^1H NMR and to 85% H_3PO_4 as an external standard for ^{31}P NMR. High-resolution mass spectra were recorded on an AutoSpec-E FISION VG mass spectrometer by chemical ionization. Nucleotides were analyzed under electron spray ionization (ESI) on a Q-TOF microinstrument (Waters, UK). $Cu(CH_3CN)_4PF_6$ was purified before use by dissolving the salt in acetonitrile (HPLC grade) and filtering the unsoluble Cu^{2+} salt by a nylon syringe 0.45 μm filter. The filtrate was deaerated with an argon stream. The concentration of the Cu^+ salt was determined by UV spectroscopy, by the addition of the specific Cu^+ indicator bicinchoninic acid disodium salt (BCA) (ε_{562} = 7700 $M^{-1}cm^{-1}$).[50] The concentration of the spin trap, DMPO in water (HPLC grade), was determined by UV spectroscopy (ε_{228} = 8000 $M^{-1}cm^{-1}$) after purification by active charcoal. Purified DMPO was stored at −20 °C subsequent to dearation with an argon stream. Analysis of OH radicals produced in Cu^+ or Fe^{2+}-H_2O_2 solutions were performed by solution EPR spectroscopy using a Bruker Elexsys 500 X-band spectrophotometer (Rheinstetten, Germany). H_2O_2 solution was purchased from Sigma Aldrich (30%) and was dissolved in HPLC-grade water to obtain the required concentration. Infrared (IR) spectra were recorded on Fourier transform infrared (FT-IR) spectrometer, using ZnSe crystal for powder samples pressed.

4.2. 2′-Deoxyguanosine-3′,5′-bisphosphorothioate, 2′-dG3′5′PS, 4. Dry 2′-deoxyguanosine (0.107 g, 0.375 mmol, 1 equiv) and dicyclohexylcarbodiimide (DCC) (1.486 g, 7.204 mmol, 19.2 equiv) were added to a two-neck round-bottom flask (25 mL) under nitrogen, in dry pyridine (2 mL). Subsequently, *S*-2-cyanoethyl phosphorothioate pyridinium salt[28] (1.200 g, 3.689 mmol, 9.8 equiv) in dry pyridine (15 mL) was added to the reaction mixture, and the latter was stirred for 3 d.[25] Water (2 mL) was added to the mixture, and the stirring continued overnight. The reaction mixture was concentrated, and the crude residue was then treated with a solution of pyridine/water (1:1), to give a white solid that was then filtered. After extraction with petroleum ether, the aqueous phase was freeze-dried to obtain an orange oil. The final product was obtained after the removal of the cyanoethyl protecting group, with potassium *tert*-butoxide (0.270 g, 2.408 mmol, 12 equiv) in the presence of ethyl mercaptane (9 mL) as acrylonitrile scavenger in THF (9 mL) for 2 h under nitrogen at RT. The product was purified on a Sephadex DEAE-A25 column applying NH_4HCO_3 buffer gradient of 0−0.2 M (100/100 mL), 0.2−0.3 M (200/200 mL), 0.5 M (300 mL), and eventually 1 M buffer (100 mL). The final purification of analogue **4** was achieved by HPLC (isocratic elution with 97% 1 M triethylammonium acetate (TEAA)/3% CH_3CN, flow rate 4 mL/min), with a retention time (Rt) of 22 min. The product was freeze-dried three times to obtain analogue **4** in 6% yield after LC (21 mg). ^1H NMR (D_2O, 600 MHz) δ (ppm): 8.32 (s, H-8, 1H), 6.39−6.37 (m, H-1′, 1H), 5.05−5.04 (m, H-3′, 1H), 4.52−4.51 (m, H-4′, 1H), 4.08−4.06 (m, H-5′, 2H), 2.87−2.82, (m, H-2′, 1H), 2.77−2.74 (m, H-2″, 1H); ^{31}P NMR (D_2O, 243 MHz) δ: 43.67 (s, 1P), 43.31 (s, 1P) ppm; ^{13}C NMR (D_2O, 151 MHz) δ (ppm): 159.98 (C-6), 154.60 (C-2), 151.43 (C-4), 137.91 (C-8), 116.12 (C-5), 86.03 (C-1′), 83.69 (C-4′), 75.43 (C-3′), 64.73 (C-5′), 38.58 (C-2′). IR (ZnSe): ν 3304, 1636, 1532, 1483, 1358, 1119, 1005, 941, 778, 615 cm^{-1}. HRMS ESI (negative) m/z: $C_{10}H_{14}N_5O_8P_2S_2^{1-}$ calcd 457.9759, found 457.9737.

4.3. Adenosine-2′,3′-bisphosphorothioate, A2′3′PS, 6. Tert-butylmagnesium chloride (1.76 mL, 1.7 M in THF, 3 mmol, 2 equiv) was added dropwise to a solution of dry 5'-O-tertbutyldimethylsilyladenosine (5′-O-TBDMSA) (0.381 g, 1.5 mmol, 1 equiv)[31] in the mixture of dry THF (20 mL) and dry DMF (1.5 mL), in a two-neck round-bottom flask (50 mL) under nitrogen. During the addition, the solution warmed up, and a white precipitate was formed. After 20 min, a solution of 2-chloro-2-thio-1,3,2-dioxaphospholane (0.158 g, 4

dx.doi.org/10.1021/ic402671q | Inorg. Chem. 2014, 53, 1594−1605

mmol, 2.66 equiv) in dry benzene (3 mL) was added. The mixture was stirred at RT for an additional 2.5 h, and the solution turned clear-yellowish. The reaction was monitored by ^{31}P NMR (the major peak of the intermediate product appeared at ~54 ppm). The solvent was evaporated, and the residue was extracted with ethyl acetate and H_2O. The organic phase was dried over Na_2SO_4, and the solvent was removed under reduced pressure to obtain a yellow liquid. A solution of NaCN (0.049 g, 12 mmol, 8 equiv) in DMSO (30 mL) was then added to the reaction mixture, and the solution was stirred overnight under vacuum (19 h). Then, the mixture was treated with NaOH (0.180 g, 4.5 mmol, 3 equiv) in EtOH (20 mL) for 2.5 h. Finally, the protecting group was removed by 1 M TBAF THF solution (1.6 mL, 1.6 mmol, respectively). Primary purification of the residue was achieved by LC on a Sephadex DEAE-A25 column. The product was eluted by the following sequence: deionized water (1 L), 0.2 M NH_4HCO_3 (1 L), 0.6 M NH_4HCO_3 (1 L), and 1 M NH_4HCO_3 (1 L). The excess buffer was removed by repeated freeze-drying cycles. The product was eluted by 0.6 M NH_4HCO_3. The resulting yellowish solid residue was further purified on a Sephadex DEAE-A25 column, applying a buffer gradient of 0.2 M NH_4HCO_3 (600 mL) to 0.6 M NH_4HCO_3 (600 mL), and eventually 1 M NH_4HCO_3 (100 mL). The final purification of compound **6** was achieved by HPLC (isocratic elution with 98% 1 M TEAA/2% CH_3CN, flow rate 1 mL/min); Rt = 3.8 min. The product was freeze-dried three times to yield 13.1 mg (4% yield) product **6**. ^1H NMR (D_2O, 600 MHz) δ (ppm): 8.43 (s, H-8, 1H), 8.30 (s, H-2, 1H), 6.37 (d, J= 6 Hz, H-1′, 1H), 5.41−5.39 (m, H2′, 1H), 5.03−5.01 (m, H-3′, 1H), 4.79 (m, H-4′, 1H signal is hidden by the water signal), 4.01−3.94 (m, H-5′, 2H); ^{31}P NMR (D_2O, 243 MHz) δ (ppm): 45.92 (s, 1P), 43.98 (s, 1P); ^{13}C NMR (D_2O, 151 MHz) δ (ppm): 155.62 (C-6), 152.29 (C-2), 148.96 (C-4), 141.59 (C-8), 119.19 (C-5), 87.40 (C-1′), 84.75 (C-4′), 74.70 (C-2′), 73.6 (C-3′), 61.58 (C-5′). IR (ZnSe): ν 3315, 1643, 1605, 1480, 1371, 1424 1215, 1125, 1023, 785, 669 cm^{-1}. HRMS ESI (negative) m/z: $C_{10}H_{14}N_5O_8P_2S_2^{1-}$ calcd 457.9759, found 457.9811.

4.4. EPR OH Radical Assay. The EPR settings for OH radical detection were as follows: microwave frequency, 9.76 GHz; modulation frequency, 100 kHz; microwave power, 6.35 mW; modulation amplitude, 1.2 G; time constant, 655.36 ms; sweep time, 83.89 s; and receiver gain, 2×10^5.

Tetrakis(acetonitrile)copper(I) hexafluorophosphate ($Cu(CH_3CN)_4PF_6$) in acetonitrile (2 mM, 5 μL) or ammonium iron(II) sulfate ($(NH_4)_2Fe(SO_4)_2$) in HPLC-grade water (1 mM, 10 μL) were added to 5−500 μM tested compound (1−10 μL) solutions. Afterward, 1 mM Tris buffer, pH 7.4, (60−68 μL) was added to the mixture. DMPO in HPLC-grade water (10 mM, 10 μL) was quickly added, followed by the addition of H_2O_2 (10 mM, 10 μL). A short mixing of the sample was performed after the addition of each component. The final pH value of the sample Fe^{2+}- or Cu^{+}-H_2O_2 systems ranged between 7.2 and 7.4. Each EPR measurement was performed 150 s after the addition of H_2O_2. The control measurement included metal ion, buffer (70−75 μL), DMPO, and H_2O_2 (excluding ligand), at the same final concentration as detailed above. All experiments were performed at RT, in a final volume of 100 μL.

4.5. Radical Scavenging Assay—Photolysis of H_2O_2. The EPR settings for OH radicals detection were as described above. The sample included 50−500 μM aqueous solution of tested compound (1−10 μL), to which 1 mM Tris buffer (70−78 μL), pH 7.4, was added. DMPO (10 mM, 10 μL) was quickly added, followed by H_2O_2 addition (10 mM, 10 μL). The sample was mixed after the addition of each component. The sample was then irradiated for 4 min with a VL-315 BL UV lamp (365 nm, 30 W, Vilber Lourmat, Marne-la-Vallée, France) and was immediately transferred to a narrow Teflon tube. The control measurement included buffer (80 μL), DMPO, and H_2O_2 (excluding ligand), at the same final concentration as detailed above. All experiments were performed at RT, in a final volume of 100 μL.

4.6. ABTS Radical Cation Decolorization Assay.[35] The ABTS radical cation ($ABTS^{\bullet+}$) was produced by reacting 7 mM aqueous ABTS stock solution with 2.45 mM potassium persulfate (final concentration) and allowing the mixture to stand in the dark at RT for 12−16 h before use. The radical was stable under these conditions for more than 2 d. The $ABTS^{\bullet+}$ solution was diluted with water, pH 7.4, to give an absorbance of 0.80 at 734 nm. After the addition of 180 μL of diluted $ABTS^{\bullet+}$ solution to 4−80 μL of tested compounds or Trolox (final concentration 5−100 μM) in water, the absorbance reading at 734 nm was taken exactly 7 min after initial mixing. Appropriate solvent blanks were measured in each assay. All determinations were carried out at least three times, in triplicate. The percentage of radical scavenging was calculated and plotted as a function of concentration of antioxidants and Trolox as the standard reference.

4.7. UV Monitoring of the Oxidation of Thiophosphate Compounds under EPR Experiment Conditions. $Cu(CH_3CN)_4PF_6$ in MeCN or $FeSO_4$ in H_2O (1 mM, 100 μL) was added to 2′-dA3′5′PS or A2′3′PS (1 mM, 100 μL) in 1 mM Tris buffer, pH 7.4 (695 μL) and H_2O_2 (10 mM, 100 μL). After 150 s, DTNB (10 mM, 5 μL) was added, to a total volume of 1 mL. Oxidation of thiophosphate compounds was monitored by UV spectroscopy (at the wavelength range of 200−600 nm) after 30 s and then in 5 min intervals for 20 min. The blank solution contained only the thiophosphate compound and DTNB in Tris buffer.

■ ASSOCIATED CONTENT

Ⓢ Supporting Information

Synthesis of compounds **1**−**4** and **6**, including NMR data for compounds **4** and **6**. This material is available free of charge via the Internet at http://pubs.acs.org.

■ AUTHOR INFORMATION

Corresponding Author

*E-mail: bilha.fischer@biu.ac.il. Tel.: 972-3-5318303. Fax: 972-3-6354907.

Notes

The authors declare no competing financial interest.

■ REFERENCES

(1) Warner, D. S.; Sheng, H.; Batinic-Haberle, I. *J. Exp. Biol.* **2004**, *207*, 3221−3231.
(2) Gilgun-Sherki, Y.; Melamed, E.; Offen, D. *Neuropharmacology* **2001**, *40*, 959−975.
(3) Fiorillo, C.; Oliviero, C.; Rizzuti, G.; Nediani, C.; Pacini, A.; Nassi, P. *Clin. Chem. Lab. Med.* **1998**, *36*, 149−153.
(4) Ha, H.; Hwang, I.-A.; Park, J. H.; Lee, H. B. *Diabetes Res. Clin. Pract.* **2008**, *82*, S42−S45.
(5) Tabner, B. J.; Turnbull, S.; King, J. E.; Benson, F. E.; El-Agnaf, O. M. A.; Allsop, D. *Free Radical Res.* **2006**, *40*, 731−739.
(6) Cherny, R. A.; Atwood, C. S.; Xilinas, M. E.; Gray, D. N.; Jones, W. D.; McLean, C. A.; Barnham, K. J.; Volitakis, I.; Fraser, F. W.; Kim, Y.-S.; Huang, X.; Goldstein, L. E.; Moir, R. D.; Lim, J. T.; Beyreuther, K.; Zheng, H.; Tanzi, R. E.; Masters, C. L.; Bush, A. I. *Neuron* **2001**, *30*, 665−676.
(7) Karmansky, I.; Gruener, N. *Clin. Chim. Acta* **1997**, *259*, 177−182.
(8) Ben-Shachar, D.; Eshel, G.; Finberg, J. P. M.; Youdim, M. B. H. *J. Neurochem.* **1991**, *56*, 1441−1444.
(9) Heinz, U.; Hegetschweiler, K.; Acklin, P.; Faller, B.; Lattmann, R.; Schnebli, H. P. *Angew. Chem., Int. Ed.* **1999**, *38*, 2568−2570.
(10) Midorikawa, K.; Murata, M.; Oikawa, S.; Hiraku, Y.; Kawanishi, S. *Biochem. Biophys. Res. Commun.* **2001**, *288*, 552−557.
(11) Sugihara, N.; Ohnishi, M.; Imamura, M.; Furuno, K. *J. Health Sci.* **2001**, *47*, 99−106.
(12) Aruoma, O. I.; Deiana, M.; Jenner, A.; Halliwell, B.; Kaur, H.; Banni, S.; Corongiu, F. P.; Dessi, M. A.; Aeschbach, R. *J. Agric. Food Chem.* **1998**, *46*, 5181−5187.
(13) Lanfer-Marquez, U. M.; Barros, R. M. C.; Sinnecker, P. *Food Res. Int.* **2005**, *38*, 885−891.
(14) Yoshioka, H.; Senba, Y.; Saito, K.; Kimura, T.; Hayakawa, F. *Biosci., Biotechnol., Biochem.* **2001**, *65*, 1697−1706.
(15) Sigel, H. *Met. Ions Biol. Syst.* **1979**, *8*, 125−158.

(16) Bloomfield, V. A.; Crothers, D. M.; Tinoco Jr., I. *Nucleic Acids: Structures, Properties, And Functions*; University Science Books: Mill Valley, CA, 2000.
(17) Richter, Y.; Fischer, B. *J. Biol. Inorg. Chem.* **2006**, *11*, 1063−1074.
(18) Baruch-Suchodolsky, R.; Fischer, B. *J. Inorg. Biochem.* **2008**, *102*, 862−881.
(19) Danino, O.; Grossman, S.; Fischer, B. *Nucleosides, Nucleotides Nucleic Acids* **2013**, *32*, 333−353.
(20) Azran, S.; Förster, D.; Danino, O.; Nadel, Y.; Reiser, G.; Fischer, B. *J. Med. Chem.* **2013**, *56*, 4938−4952.
(21) Sayer, A. H.; Itzhakov, Y.; Stern, N.; Nadel, Y.; Fischer, B. *Inorg. Chem.* **2013**, *52*, 10886−10896.
(22) Yoshikawa, M.; Kato, T.; Takenishi, T. *Bull. Chem. Soc. Jpn.* **1969**, *42*, 3505−3508.
(23) Knorre, D.; Lebedev, A.; Zarytova, V. *Nucleic Acids Res.* **1976**, *3*, 1401−1418.
(24) Camaioni, E.; Boyer, J. L.; Mohanram, A.; Harden, T. K.; Jacobson, K. A. *J. Med. Chem.* **1998**, *41*, 183−190.
(25) Bennett, G.; Gough, G.; Gilham, P. *Biochem.* **1976**, *15*, 4623−4628.
(26) Tener, G. *J. Am. Chem. Soc.* **1961**, *83*, 159−168.
(27) Maciej, S. B.; Désaubry, L.; Johnson, R. A. *Tetrahedron Lett.* **1998**, *39*, 7455−7458.
(28) Burgers, P. M.; Eckstein, F. *Biochemistry* **1979**, *18*, 592−596.
(29) Stec, W. J.; Grajkowski, A.; Kobylanska, A.; Karwowski, B.; Koziolkiewicz, M.; Misiura, K.; Okruszek, A.; Wilk, A.; Guga, P.; Boczkowska, M. *J. Am. Chem. Soc.* **1995**, *117*, 12019−12029.
(30) Cooke, A. M.; Potter, B. V. L; Gigg, R. *Tetrahedron Lett.* **1987**, *28*, 2305−2308.
(31) Shen, W.; Kim, J.-S.; Mitchell, S.; Kish, P.; Kijek, P.; Hilfinger, J. *Nucleosides, Nucleotides Nucleic Acids* **2009**, *28*, 43−55.
(32) Finkelstein, E.; Rosen, G. M.; Rauckman, E. J. *Arch. Biochem. Biophys.* **1980**, *200*, 1−16.
(33) Anzai, K.; Aikawa, T.; Furukawa, Y.; Matsushima, Y.; Urano, S.; Ozawa, T. *Arch. Biochem. Biophys.* **2003**, *415*, 251−256.
(34) Ikai, H.; Nakamura, K.; Shirato, M.; Kanno, T.; Iwasawa, A.; Sasaki, K.; Niwano, Y.; Kohno, M. *Antimicrob. Agents Chemother.* **2010**, *54*, 5086−5091.
(35) Re, R.; Pellegrini, N.; Proteggente, A.; Pannala, A.; Yang, M.; Rice-Evans, C. *Free Radical Biol. Med.* **1999**, *26*, 1231−1237.
(36) Izatt, R. M.; Christensen, J. J.; Rytting, J. H. *Chem. Rev.* **1971**, *71*, 439−481.
(37) Martin, R. B.; Mariam, Y. H. *Met. Ions Biol. Syst.* **1979**, *8*, 57−124.
(38) Scheller, K. H.; Hofstetter, F.; Mitchell, P. R.; Prijs, B.; Sigel, H. *J. Am. Chem. Soc.* **1981**, *103*, 247−260.
(39) Scheller, K. H.; Sigel, H. *J. Am. Chem. Soc.* **1983**, *105*, 5891−5900.
(40) Sigel, H.; Massoud, S. S.; Tribolet, R. *J. Am. Chem. Soc.* **1988**, *110*, 6857−6865.
(41) Martin, R. B. *Acc. Chem. Res.* **1985**, *18*, 32−38.
(42) Sigel, H.; Griesser, R. *Chem. Soc. Rev.* **2005**, *34*, 875−900.
(43) Mitchell, P. R.; Sigel, H. *Eur. J. Biochem.* **1978**, *88*, 149−154.
(44) Sigel, H.; Tribolet, R.; Malini-Balakrishnan, R.; Martin, R. B. *Inorg. Chem.* **1987**, *26*, 2149−2157.
(45) Sigel, R. K.; Song, B.; Sigel, H. *J. Am. Chem. Soc.* **1997**, *119*, 744−755.
(46) Chatterji, D.; Nandi, U.; Podder, S. *Biopolymers* **1977**, *16*, 1863−1878.
(47) Voet, D.; Gratzer, W.; Cox, R.; Doty, P. *Biopolymers* **1963**, *1*, 193−208.
(48) Bosque-Sendra, J. M.; Almansa-Lopez, E.; Garcia-Campana, M.; Cuadros-Rodriguez, L. *Anal. Sci.* **2003**, *19*, 1431−1439.
(49) Marzilli, L. G.; De Castro, B.; Caradonna, J. P.; Stewart, R. C.; Van Vuuren, C. *J. Am. Chem. Soc.* **1980**, *102*, 916−924.
(50) Brenner, A. J.; Harris, E. D. *Anal. Biochem.* **1995**, *226*, 80−84.